Supporting Information

3D graphene decorated with nickel nanoparticles: in-situ synthesis, enhanced dispersibility, and absorption-dominated electromagnetic interference shielding

Liqing Chen,[a, b, c] *Nian Li,*[a, c, *] *Xinling Yu,*[a, d] *Cui Liu,*[a, c] *Yanping Song,*[a, b, c] *Zhao Li,*[a, b, c] *Jun Kang,*[a, c] *Wenbo Wang,*[a, b, c] *Na Hong,*[a, b, c] *Hu Ge,*[a, d] *Pengzhan Yang,*[a, b, c] *Shudong Zhang,*[a, c, *] *and Zhenyang Wang.* [a, c, *]

[a] Institute of Solid-State Physics, Chinese Academy of Sciences, Hefei, Anhui 230031, China

[b] Department of Chemistry, University of Science and Technology of China, Hefei, Anhui 230026, China

[c] Key Laboratory of Photovoltaic and Energy Conservation Materials, Hefei Institutes of Physical Science, Chinese Academy of Sciences, Hefei 230031, China

[d] School of Advanced Manufacturing Engineering, Hefei University, Hefei, Anhui 230601, China

* Corresponding authors. E-mail: linian@issp.ac.cn (Nian Li); sdzhang@iim.ac.cn (Shudong Zhang); zywang@iim.ac.cn (Zhenyang Wang).

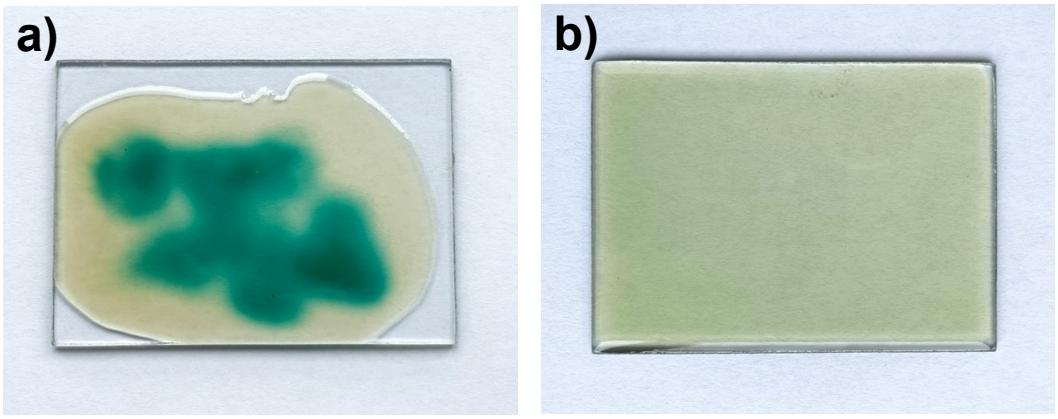

Fig. S1. The image of PI/Ni(II) on the glass plate obtained by thermal curing of $NiCl_2$ in (a) PAA and (b) PAA-COOH.

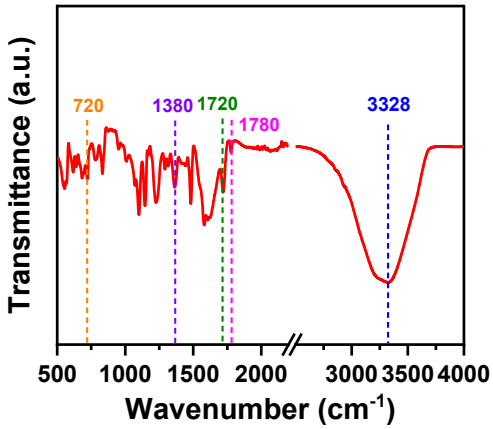

Fig. S2. FTIR spectrum of PI containing Ni(II).

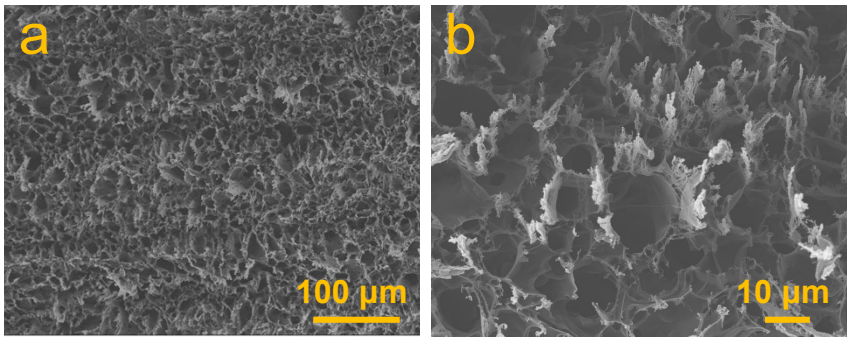

Fig. S3. (a, b) Top view SEM images of LIG/Cu.

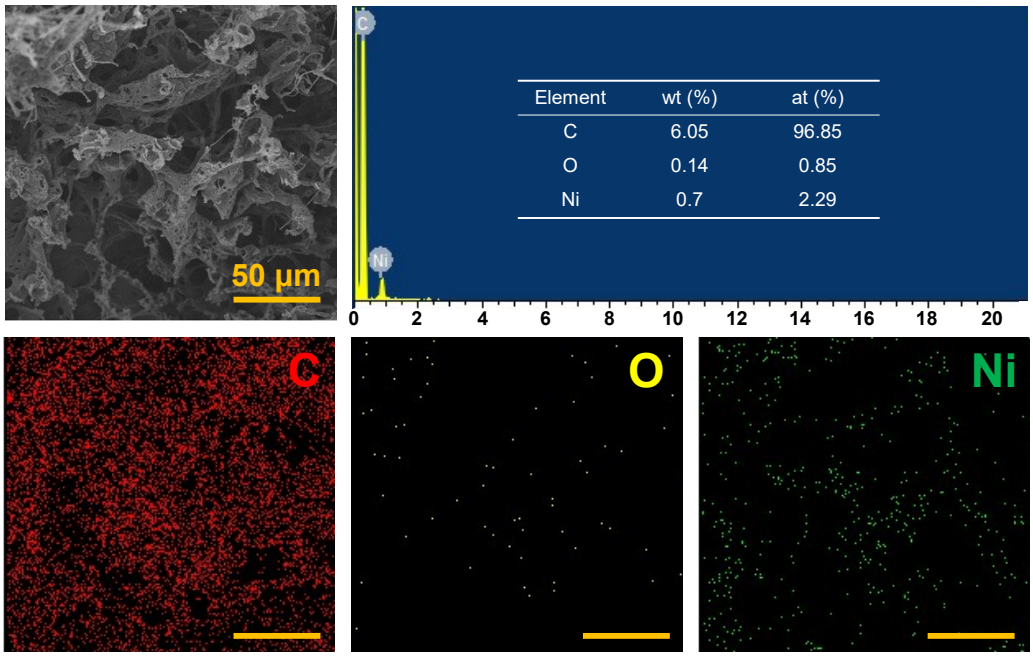

Fig. S4. SEM EDS elemental mappings of LIG/Ni.

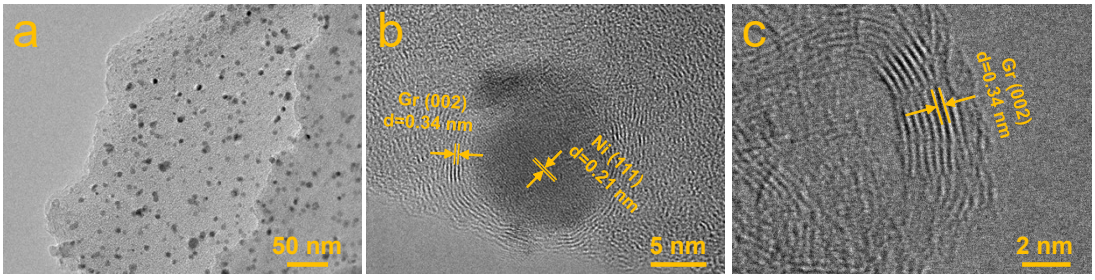

Fig. S5. (a) TEM image and (b, c) High-resolution TEM images of LIG/Ni.

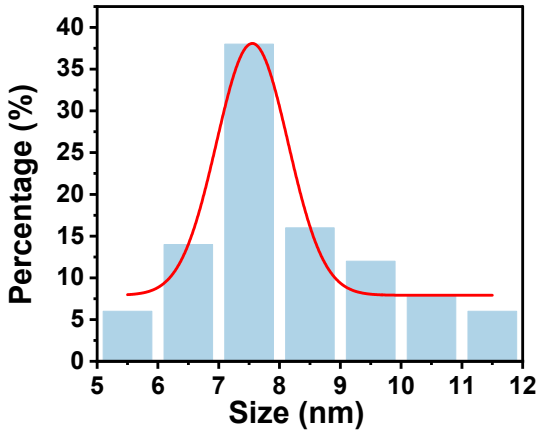

Fig. S6. Size distribution of Ni nanoparticles.

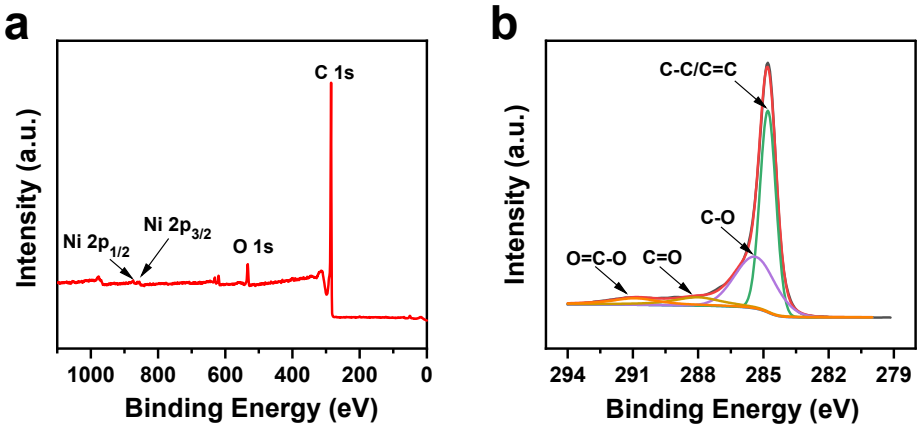

Fig. S7. (a) Full XPS spectrum of LIG/Ni. (b) High-resolution C 1s spectrum of LIG/Ni.

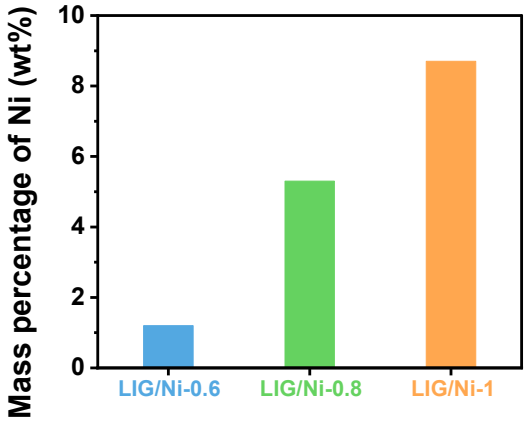

Fig. S8. Mass percentage of Ni for different samples.

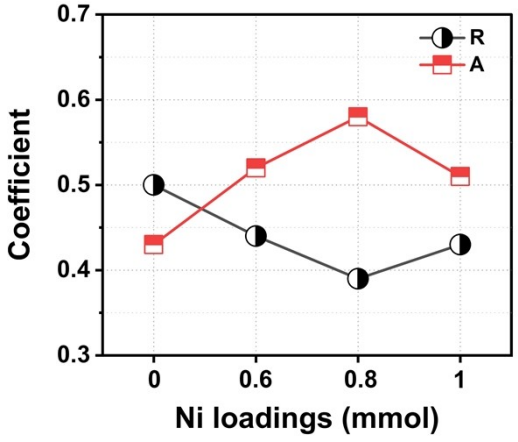

Fig. S9. A-R coefficients of different samples.

Fig. S10. Mechanical flexibility test of LIG/Ni.

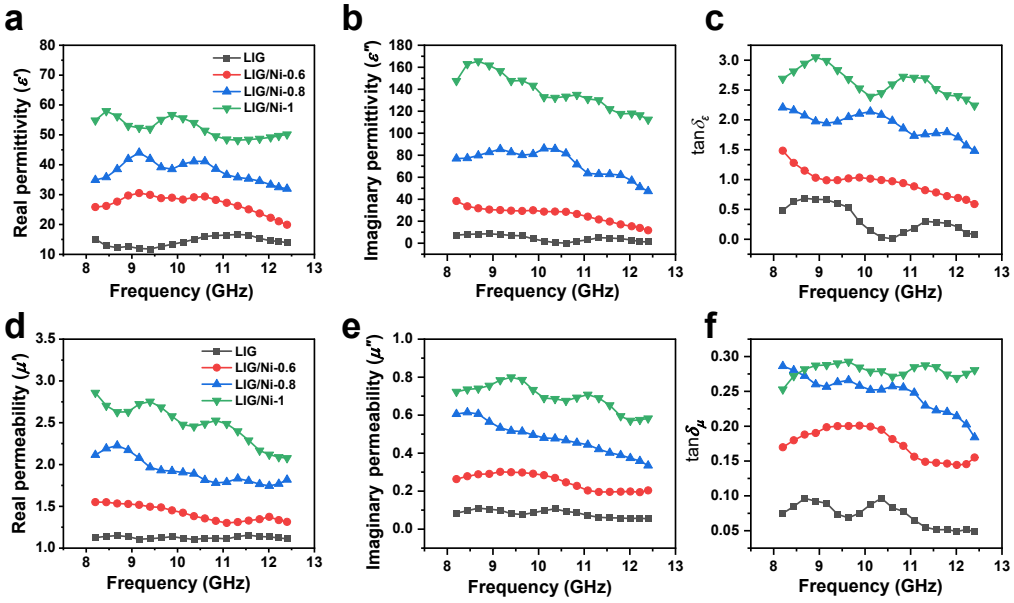

Fig. S11. (a-b) Complex permittivity and (c) dielectric loss of LIG/Ni with different Ni contents; (d-e) The complex permeability and (f) magnetic loss of LIG/Ni with different Ni contents.

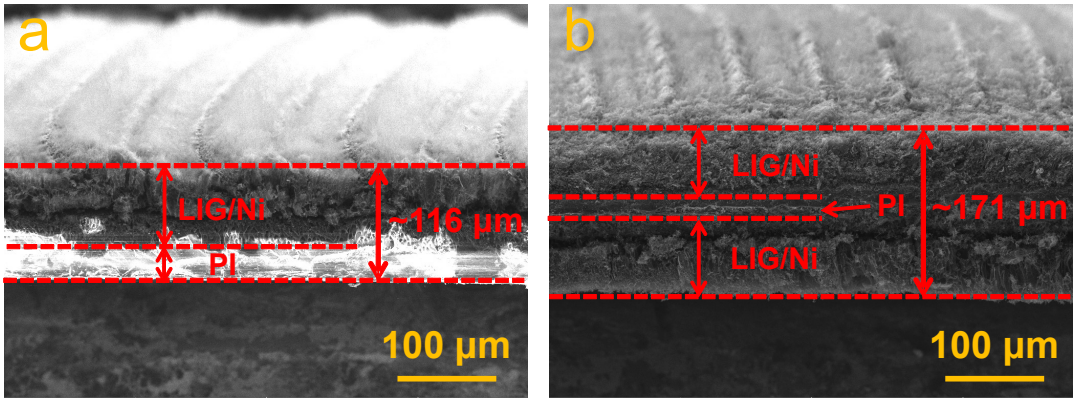

Fig. S12. Cross-sections SEM images of (a) LIG/Ni-0.8 and (b) D-LIG/Ni-0.8.

Table S1. Comparison of the EMI shielding performance (in the X-band) of the reported 3D carbon-based shielding materials in terms of filler content and thickness.

Sample	Filler Content (wt%)	Thickness (mm)	EMI SE_T (dB)	Ref.
FeNi/CNT	30	1.4	35.7	1
Fe_3O_4@graphene foam/PDMS foam	7.1	1	32.4	2
Fe_3O_4/Graphene paper	50	0.3	22	3
LIG/Fe_3O_4	10	0.053	32.7	4
GF/h-Fe_3O_4/PDMS	12	2	70.37	5
rGO/MWCNT/PDMS	0.98	2.4	56	6
CNTs@PAN–Fe_3O_4 fibers	10	2	80	7
Fe_3O_4@MWCNT/RGO paper	3.2	0.6	45.9	8
FCC-GF-PDMS	13	1	48	9
Ni@graphene-PVDF	10	0.7	51.4	10
Ni@porous carbon composite	28.76	2	48.7	11
D-LIG/Ni-0.8	5.3	0.171	94	This work

References:

1 Menon, A. V.; Madras, G.; Bose, S. Magnetic Alloy-Mwnt Heterostructure as Efficient Electromagnetic Wave Suppressors in Soft Nanocomposites. *Chemistry Select* **2017**, *2*, 7831-7844.

2 Zhu, S.; Cheng, Q.; Yu, C.; Pan, X.; Zuo, X.; Liu, J.; Chen, M.; Li, W.; Li, Q.; Liu, L. Flexible

Fe3o4/Graphene Foam/Poly Dimethylsiloxane Composite for High-Performance Electromagnetic Interference Shielding. *Compos. Sci. Technol.* **2020**, *189*, 108012.

3 Song, W.-L.; Guan, X.-T.; Fan, L.-Z.; Cao, W.-Q.; Wang, C.-Y.; Zhao, Q.-L.; Cao, M.-S. Magnetic and Conductive Graphene Papers toward Thin Layers of Effective Electromagnetic Shielding. *J. Mater. Chem. A* **2015**, *3*, 2097-2107.

4 Yu, W.; Peng, Y.; Cao, L.; Zhao, W.; Liu, X. Free-Standing Laser-Induced Graphene Films for High-Performance Electromagnetic Interference Shielding. *Carbon* **2021**, *183*, 600-611.

5 Fang, H.; Guo, H.; Hu, Y.; Ren, Y.; Hsu, P.-C.; Bai, S.-L. In-Situ Grown Hollow Fe3o4 onto Graphene Foam Nanocomposites with High Emi Shielding Effectiveness and Thermal Conductivity. *Compos. Sci. Technol.* **2020**, *188*, 107975.

6 Jia, H.; Kong, Q.-Q.; Liu, Z.; Wei, X.-X.; Li, X.-M.; Chen, J.-P.; Li, F.; Yang, X.; Sun, G.-H.; Chen, C.-M. 3d Graphene/ Carbon Nanotubes/ Polydimethylsiloxane Composites as High-Performance Electromagnetic Shielding Material in X-Band. *Compos. Part A-Appl. S* **2020**, *129*, 105712.

7 Wei, H.; Zheng, W.; Jiang, Z.; Huang, Y. Cnt Coatings Grown on the Outer and Inner Surfaces of Magnetic Hollow Carbon Fibers with Enhanced Electromagnetic Interference Shielding Performance. *J. Mater. Chem. C* **2019**, *7*, 14375-14383.

8 Zhou, J.; Tao, H.; Xia, L.; Zhao, H.; Wang, Y.; Zhan, Y.; Yuan, B. An Innovative Ternary Composite Paper of Graphene and Fe3o4 Decorated Multi-Walled Carbon Nanotube for Ultra-Efficient Electromagnetic Interference Shielding and Fire-Resistant Properties. *Compos. Commun.* **2022**, *32*, 101181.

9 Yu, C.; Zhu, S.; Xing, C.; Pan, X.; Zuo, X.; Liu, J.; Chen, M.; Liu, L.; Tao, G.; Li, Q. Fe Nanoparticles and Cnts Co-Decorated Porous Carbon/Graphene Foam Composite for

Excellent Electromagnetic Interference Shielding Performance. *J. Alloys Compd.* **2020**, *820*, 153108.

10 Liang, L.; Xu, P.; Wang, Y.; Shang, Y.; Ma, J.; Su, F.; Feng, Y.; He, C.; Wang, Y.; Liu, C. Flexible Polyvinylidene Fluoride Film with Alternating Oriented Graphene/Ni Nanochains for Electromagnetic Interference Shielding and Thermal Management. *Chem. Eng. J.* **2020**, *395*, 125209.

11 Zheng, Y.; Song, Y.; Gao, T.; Yan, S.; Hu, H.; Cao, F.; Duan, Y.; Zhang, X. Lightweight and Hydrophobic Three-Dimensional Wood-Derived Anisotropic Magnetic Porous Carbon for Highly Efficient Electromagnetic Interference Shielding. *ACS Appl. Mater. Interfaces* **2020**, *12*, 40802-40814.